HIGH POWER SECOND HARMONIC GENERATION OF 257 nm RADIATION IN AN EXTERNAL RING CAVITY

J.C. BERGQUIST, Hamid HEMMATI and Wayne M. ITANO
Time and Frequency Division, National Bureau of Standards, Boulder, CO 80303, USA

Received 30 August 1982

Continuous wave high power frequency doubling of a stabilized, single mode argon ion laser in a resonant external ring cavity is discussed and experimental results are presented. The second harmonic is generated in a Brewster cut ADP crystal which is 90° temperature phase matched. Greater than 80 milliwatts of stable, usable radiation at 257 nm is generated. Successful operation of the ring cavity with an internal harmonic beamsplitter to extract the UV radiation is reported.

1. Introduction

Continuous wave ultraviolet lasers are important in many areas of physics, including high resolution spectroscopy and radiatively cooled stored ions (whose first resonance lines are frequently in the UV). The generation of narrowband, tunable UV radiation near 194 nm is of particular interest to us in our spectroscopic studies of laser cooled mercury ions (Hg^+). The optimum cooling transition in Hg^+, which is an attractive candidate for ultra high resolution frequency and time metrology [1–3], is the first resonance line at 194.2 nm. The generation of tunable 194 nm is possible by the sum frequency mixing of doubled 514 nm (257 nm) and 792 nm radiation in potassium pentaborate (KB5) [4,5] which can be 90° phase matched at ~35°C. To achieve suitable power levels at 194 nm, ($\gtrsim 10^{-6}$ W) it is desirable to begin with $\gtrsim 0.1$ W at 257 nm. A simple and efficient method to generate single frequency 257 nm radiation is to insert a Brewster cut doubling crystal in an external ring cavity which is electronically servoed to resonance with a single mode argon ion laser at 514 nm.

Ashkin et al. [6] first presented some of the attributes of the external passive linear cavity with regard to enhanced second harmonic generation. Dunn and Ferguson [7] discussed methods to correctly compensate for the astigmatism and coma which are introduced by intracavity Brewster cut doubling crystals that are necessarily located in a tight waist. These ideas are directly extendible to external ring cavities. Recently, and concurrent with our effort at NBS with external ring cavities, Brieger et al. [8] reported efficient frequency doubling of a stabilized, single mode, cw dye laser in a passive ring cavity. In the latter experiment the cavity was not locked to the fundamental laser frequency, but was only swept through resonance. From this, they observed a fundamental power build up of approximately 15 and a corresponding, nearly ideal, second harmonic power enhancement of ~225. As discussed elsewhere in the literature [9,10], thermal gradients in the crystal can present realization of the ideal fundamental-wavelength power squared enhancement factor.

In this paper, we report our experimental results obtained with a resonant external ring cavity used to frequency double the 514.5 nm radiation from a single mode stabilized argon ion laser. As much as 80 milliwatts of stable, continuous wave power at 257.3 nm is generated in a 45° Z-cut, 90° temperature phase matched ammonium dihydrogen phosphate (ADP) crystal. The UV radiation is extracted from the ring resonator by means of a second harmonic beamsplitter which reflects 99.8% of the UV but is highly transparent to the fundamental radiation. Since the dichroic beamsplitter preserves the high intracavity fundamental power, this method appears to be a better alternative to the method of UV extraction by partially transmitting mirrors, which are lossy and sometimes damaged by absorption of the UV radiation.

The fundamental circulating power, P_c, in a mode matched ring cavity that is servo locked to resonance is related to the input power P_i by the following formula [6]

$$P_c \simeq P_i(1-R)/(1-\sqrt{R(1-L)})^2,$$

where L is the power loss factor per round trip in the cavity. The parameter L contains all linear power loss terms including the crystal and mirror scattering and absorption losses. R is the power reflection coefficient of the input mirror. The circulating power is maximum when R is set equal to unity minus the loss factor per pass, $1-L$, and is simply given by

$$P_c \simeq P_i/(1-R) \simeq P_i/L.$$

As expected, a low loss factor can lead to a significant circulating power in an external cavity. Elsewhere [11], based solely on fundamental power enhancement arguments, it is shown that second harmonic generation in an external cavity is equal to or superior to laser intracavity frequency doubling in most instances. If the additional advantages of an external ring cavity are considered, such as simplicity of design and construction, single direction for fundamental and UV radiation in the crystal, simpler laser operation, etc., the ring cavity is a compelling alternative to laser intracavity doubling.

The second harmonic power P_2 generated in the ADP crystal is given by $P_2 = KP_c^2$ where K is the nonlinear conversion coefficient. The coefficient K depends on internal crystal parameters, crystal length, the wavelength of the fundamental radiation, the index matching function and optical beam geometry. K also includes any thermal lensing, absorption and scattering effects which have a functional dependence on P_c and P_2. For sufficiently high powers the thermal gradients established in the crystal by the absorption of fundamental radiation leads to a linear rather than a quadratic dependence of second harmonic power on fundamental power [9,10]. In the low power limit typical values for the ADP crystals which we have tried range from $(6-14) \times 10^{-4}\ \mathrm{W}^{-1}$.

2 Experimental

The experimental set up for second harmonic generation of the single frequency output of an iodine stabilized Ar^+ laser is shown in fig. 1. Single mode operation of the Ar^+ laser is achieved with a 10 mm, solid, temperature tuned etalon. Frequency tuning and stabilization of the laser is made possible by mounting the laser's high reflecting back mirror on a piezo-electric transducer (PZT). The Ar^+ laser is short term stabilized by locking the laser to the half power point of a stable transfer cavity [12]. The laser is frequency modulated and long term stabilized by a first derivative lock of the transfer cavity to the saturated absorption feature of a nearby iodine line [13–15]. Two approx-

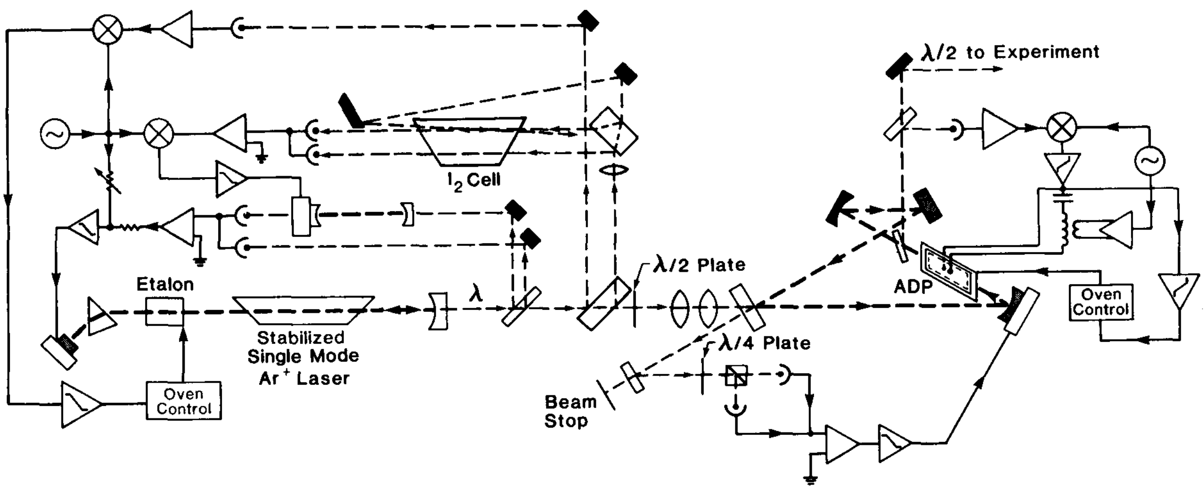

Fig. 1. Experimental set up for generation of 257 nm radiation in an external ring cavity.

imately equal amplitude probe beams from an uncoated beamsplitter are passed through the iodine cell, only one of which is crossed at a small angle by the saturating beam. The probe beams are differentially detected to eliminate intensity noise [15] and offsets due, e.g., to phase sensitive detection of the Doppler background or of the thick etalon. Long-term frequency stabilization of the thick etalon is done by phase sensitively detecting the amplitude modulation of the laser and feeding back to the etalon through the temperature controller.

The laser output is mode matched into a four mirror ring resonator which contains the Brewster cut ADP doubling crystal and harmonic beamsplitter. As mentioned above, the optimum circulating power is achieved when the transmission of the input coupler is equal to the total round trip cavity losses. Empirically, these losses vary from 3 to 12% largely dependent on the ADP crystal quality. Therefore, we have a choice of plano input couplers with power reflectivities of 97%, 95% and 89% that permit empirical optimization of the cavity power. The remaining three mirrors are highly reflecting ($\gtrsim 99.7\%$) at the fundamental wavelength. Two of the highly reflecting mirrors, with a common radius of curvature of 30 cm, combine to focus and recollimate the circulating radiation. The fourth mirror is plano. It is possible to select the mirror radii of curvature and adjust the cavity length, L, to obtain the optimum spot size, w_0, in a crystal of length, $l (l\lambda/2\pi w_0^2 = 2.84)$ [16]. It is also possible to select the mirror radii of curvature and the opening angle required to correctly compensate for both astigmatism and coma [7]. Finally it is possible, but practically difficult, to match the mirror radii of curvature that simultaneously satisfy both criteria. For ADP and a common radius of curvature (R_0) for the two curved mirrors, this match occurs for $0.56R_0 \simeq l \simeq 0.16L$. In our compromise, the ring cavity is correctly compensated for astigmatism but not for coma. The spot size is nearly optimum ($\sim 50\ \mu$m) for the ADP crystal length of 5 cm used in these experiments.

The UV radiation at 257 nm was extracted from the cavity by means of a dielectric second harmonic beamsplitter which was coated to reflect 99.8% of the S-polarized second harmonic beam at an angle of incidence of 45°. The harmonic beamsplitter was hand selected to transmit $\gtrsim 98\%$ of the P-polarized fundamental radiation. The beamsplitter is placed immediately after the crystal to prevent the UV radiation from reaching any mirror. This not only prevents UV damage to the mirror coatings, but also eases the coating requirements to be strictly highly reflecting for the fundamental rather than a coating that is transmitting in the UV and highly reflecting for the fundamental frequency. For dichroic mirrors the UV transmission is usually less than 80% (typically 60–70%). Additionally, it should be possible to coat highly reflecting second harmonic beamsplitters which would have close to unit transmission for the fundamental. Perhaps Brewster's angle for the fundamental wavelength on a properly coated beamsplitter could improve the fundamental power transmission coefficient beyond 99%. The thickness of the beamsplitter is 6.4 mm which adds little aberration to the fundamental beam quality beyond that of the nonlinear crystal and is easily compensated for.

The ADP crystal must be cooled to approximately -10°C in order to achieve 90° phasematching of the 514.5 nm Ar^+ line [17]. To facilitate temperature tuning, the crystal is mounted in a 50 mm × 50 mm × 12 mm copper housing which provides a reasonably uniform thermal bath. This copper block is attached to a Peltier cooler that is heat sunk into a larger water cooled copper block. The time constant for a small temperature change is on the order of a few seconds. Several methods have been successfully used to prevent water vapor condensation on the cooled crystal faces. In one method dry nitrogen is continuously flowed over the crystal faces. In another scheme the crystal and cooler are placed in a small housing which is evacuated and back filled with either dry argon or helium. In vacuum, the poor contact of the copper block to the crystal prevented efficient and uniform heat transfer, but we expect that use of a copper or gold sponge would eliminate this problem. Our housing uses a Brewster-angled input window and the dichroic beamsplitter as the output window for the fundamental radiation. The UV radiation is reflected from the beamsplitter and exits the housing through a UV grade synthetic quartz, Brewster-angled window (oriented for the UV) which prevents any further Fresnel losses.

Temperature regulation to 10 mK is done with thermistors attached to the crystal housing. We attempted fine "temperature" stabilization of the crystal for optimization of the 90° phase match condition by fast electrooptic tuning of the ADP crystal [18,19]. This method permits fast, but limited, compensation for small temperature deviations from the 90° phase match condition, but does not correct for temperature gradients across the crystal. Copper clad tape was mounted to the two faces of the crystal normal to the crystal's optic axis (thereby normal to the E field direction of the second harmonic radiation). Introduction of a voltage difference between the two plates produces an electric field in the crystal which induces an index of refraction change for the fundamental radiation. Experimentally, the available 0–2 kilovolt voltage amplifier compensates for temperature fluctuations in the crystal which do not exceed 0.08°C. In order to servo the crystal to the optimal phase match condition, a 30 kHz, 300 V peak-to-peak AC voltage is applied to the crystal by means of an audio transformer to permit phase sensitive detection and a first derivative lock. This modulation depth causes an indiscernible cavity optical length change and thereby does not affect the lock of the cavity to the fundamental. In the future we expect to follow this loop with a slower integrator to the crystal temperature controller.

The stabilization of the ring cavity to the laser is accomplished by the polarization technique discussed by Hänsch and Couillaud [20] and proposed for this application by Brieger et al. [8]. In this scheme, the dispersive resonances of the cavity are analyzed in the cavity reflected laser beam by means of a $\lambda/4$ wave plate and a linear polarizer. The dispersive resonances were produced by slightly rotating the polarization of the input laser beam with respect to the polarization defined by the crystal Brewster faces by means of a high quality zero order, antireflection coated, $\lambda/2$ plate. Typically ~5° of rotation produced sufficiently strong signals to servo lock the cavity for an indefinite period of time. As pointed out in ref. [20], the dispersive resonance provides signal information far into the wings away from the line center, enabling the ring cavity to acquire and automatically relock to the original cavity order even against severe environmental perturbations.

The enhancement factor of the cavity is measured by comparing the fundamental power which "leaks" through one of the highly reflecting mirrors when the cavity is on resonance to the power which leaks through the same mirror with the input coupler removed. The fundamental power enhancement factor ranges from 8–25 with the ADP crystals which we have. The UV radiation is passed through an uncoated beamsplitter in order to split off a calculable fraction of the UV radiation for power measurements on a calibrated PIN diode.

3. Results

The optimum aberration compensating opening angle was empirically determined with a good quality, plane parallel glass substrate substituted for the ADP crystal. As might be expected, the correct compensation angle for astigmatism provided a greater cavity power enhancement factor than the compensation angle for coma. However, the theoretically predicted opening angles for both angles produced local maxima in cavity power buildup. With the glass substrate, a maximum fundamental enhancement factor of ~33 was achieved with a 97% reflecting input coupler and without mode matching. This implied a total round trip loss factor of ~3%. Substitution of the 5 cm long Brewster cut ADP crystal and the harmonic beamsplitter for the glass substrate reduced the power enhancement factor, even after mode matching and reoptimization of the cavity compensation angle and input coupler. For the ADP crystal with the lowest insertion loss the maximum fundamental power enhancement factor with mode matching is ~25, more typically ~20. The principal limit to the power buildup factor is probably due to the surface and bulk crystal losses.

With as much as 2.0 W of single frequency power coupled into the ring cavity, and in the absence of UV generation, we maintain a fairly constant fundamental power enhancement of approximately 20. However, when the crystal is temperature tuned to the 90° phase matched condition so that 257 nm radiation is generated, the cavity circulating power decreases to a smaller value. This decrease probably results from losses due to thermal lensing effects and not from the power loss due to conversion of fundamental to UV radiation. This process is reversible; heating the crystal restores the original power enhancement factor. With, for example, 2 W of 514.5 nm radiation coupled into the ring cavity the power enhancement drops approximately 25% from ~20 to ~15 when the crystal is tuned to the optimum UV generation temperature. In our best crystal, 20 W of circulating power produces 80 mW of stable, cw radiation at 257 nm. If the Fresnel scattering losses at the exit face of the crystal are included, the total UV power generated is about 94 mW. This UV power represents a loss factor per pass of less than 0.5% of the fundamental circulating power, and thereby accounts for no more than a small fraction ($\lesssim$16%) of the precipitous drop in the fundamental power enhancement.

The 94 mW of UV radiation is below the power predicted by the square law fundamental power dependence and the low power harmonic conversion coefficient of 6×10^{-4} W^{-1}. As previously mentioned, this difference is partly attributable to the transverse phase mismatch caused by the thermal gradients established in the crystal by the absorption of fundamental radiation and/or the absorption of UV and fundamental radiation. In ref. [9] this departure of second harmonic power from quadratic dependence on fundamental power is explained in terms of self-induced thermal phase mismatching due to the absorption of fundamental power in the crystal. The nonuniform heating due to the gaussian beam profile of the fundamental beam together with the crystal finite heat conductivity leads to a nonuniform temperature profile across the beam. This prevents transverse phase matching across the entire beam. This model predicts that the generated second harmonic power will grow linearly proportional to the fundamental power for sufficiently high fundamental power.

Fig. 2 shows a logarithmic plot of UV power generated versus circulating fundamental power for two of our crystals. The Fresnel loss at the crystal exit face is included. The deviation from square law dependence is evident, but the reduction in second harmonic power is markedly worse than the crossover to linear dependence predicted above. The empirical fact that the presence of the UV radiation strongly reduces the fundamental circulating power suggests that additional processes, such as UV and/or multiphoton absorption, should be included in order to better model the strong departure from quadratic dependence.

In the future, we plan to try other crystals from various vendors and of various lengths. Ferguson and Dunn [21] find a soft function of second harmonic efficiency versus crystal length for a given circulating fundamental power. The optimum crystal length from their argument gives a factor of three shorter crystal than our present 5 cm length. The Rice University group [22] found that the longer the intracavity crystal the better the second harmonic power, but the variance in crystal quality may explain this behavior.

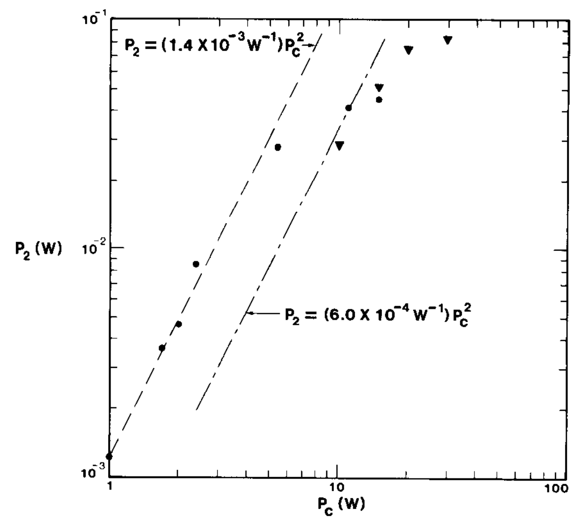

Fig. 2. Logarithmic plot showing second harmonic power versus fundamental circulating power for two ADP crystals (●●●, crystal A; ▲▲▲, crystal B). The dashed lines show the second harmonic power predicted from the product of fundamental power squared times the low power, nonlinear conversion coefficient, K (——— ———, crystal A; ——•——, crystal B).

We wish to thank our colleagues R.E. Drullinger, C.R. Pollock and D.J. Wineland for many stimulating and useful conversations. We gratefully acknowledge the support of the United States Air Force Office of Scientific Research and the Office of Naval Research.

References

[1] F.G. Major and G. Werth, Phys. Rev. Lett. 30 (1973) 1155; Appl. Phys. 15 (1978) 201.
[2] P.L. Bender, J.L. Hall, R.H. Garstang, F.M.J. Pichanick, W.W. Smith, R.L. Barger and J.B. West, Bull. Am. Phys. Soc. 21 (1976) 599.
[3] D.J. Wineland, W.M. Itano, J.C. Bergquist and F.L. Walls, Proc. 35th Ann. Symp. on Frequency control (U.S. Army Electronics Command, Fort Monmouth, NJ 1981) p. 602.
[4] R.E. Stickel Jr. and F.B. Dunning, Appl. Optics 17 (1978) 981.
[5] H. Hemmati, J.C. Bergquist and W.M. Itano, Proc. Topical Meeting on Laser techniques for extreme ultraviolet spectroscopy (Am. Institute of Phys. 1982).
[6] A. Ashkin, G.C. Boyd and J.M. Dziedzic, IEEE J. Quantum Electron. QE-2 (1966) 109.
[7] M.H. Dunn and A.I. Ferguson, Optics Comm. 20 (1977) 214.

[8] M. Brieger, A. Büsener, A. Hese, F.V. Moers and A. Renn. Optics Comm. 38 (1981) 423.
[9] M. Okada and S. Leiri, IEEE J. Quantum Electron. QE-7 (1971) 469.
[10] A.I. Ferguson, M.H. Dunn and A. Maitland, Optics Comm. 19 (1977) 10.
[11] J.C. Bergquist, submitted for publication.
[12] R.L. Barger, M.S. Sorem and J.L. Hall, Appl. Phys. Lett. 22 (1973) 573.
[13] F. Spieweck, Appl. Phys. 3 (1974) 429.
[14] G. Camy, B. Decomps, J.L. Gardissat and C.J. Bordé, Metrologia 13 (1971) 145.
[15] T.W. Hänsch, I.S. Shahin and A.L. Schawlow, Phys. Rev. Lett. 27 (1971) 707.
[16] G.D. Boyd and D.A. Kleinman, J. Appl. Phys. 39 (1968) 3597.
[17] P. Huber, Optics Comm. 15 (1975) 196;
M.W. Dowley, Appl. Phys. Lett. 13 (1968) 395.
[18] N.I. Adams, III and J.J. Barrett, IEEE J. Quantum Electron. QE-2 (1966) 430.
[19] David T. Hon, IEEE J. Quantum Electron. QE-12 (1976) 148.
[20] T.W. Hänsch and B. Couillaud, Optics Comm. 35 (1980) 441.
[21] A.I. Ferguson and M.H. Dunn. IEEE J. Quantum Electron. QE-13 (1977) 751.
[22] C.R. Pollock, private communication.